Journal of The Electrochemical Society, **150** (5) F97-F101 (2003)
0013-4651/2003/150(5)/F97/5/$7.00 © The Electrochemical Society, Inc.

How Pore Size and Surface Roughness Affect Diffusion Barrier Continuity on Porous Low-*k* Films

Jia-Ning Sun,[a] Yifan Hu,[a] William E. Frieze,[a] Wei Chen,[b] and David W. Gidley[a,z]

[a]*Department of Physics, University of Michigan, Ann Arbor, MI 48109, USA*
[b]*Dow Corning, Midland, MI 48686, USA*

The structural features that affect continuity of ultrathin diffusion barriers on porous low-dielectric-constant (*k*) thin films has been investigated. The dimensions of interconnected nanopores in a series of Dow Corning XLK films are found to increase as the dielectric constant becomes smaller. The minimum thickness required for tantalum (Ta) to form a continuous barrier layer is affected by the pore size and surface roughness of the porous low-*k* films according to positronium annihilation lifetime spectroscopy analysis. The films with large pores require thick barrier layers to form effective diffusion barriers. The surface roughness of the porous films as observed by atomic force microscopy has a significant influence on the continuity of diffusion barriers.
 [DOI: 10.1149/1.1566415]

Manuscript submitted June 6, 2002; revised manuscript received November 25, 2002. Available electronically March 20, 2003.

The integration of copper with porous ultralow-*k* interlayer dielectrics (ILDs) has attracted significant interest because the combination will lead to additional performance improvement in reducing the resistance-capacitance (RC) time delay of integrated circuits.[1] However, Cu is known to have high diffusivity into most of the promising ILD materials, and the presence of Cu in the pores of low-*k* materials results in serious device degradation and failure. Therefore, it is necessary to separate the Cu interconnect lines from the surrounding ILD by thin liner/barrier layers.[2]

The liner materials must satisfy a number of diverse specifications, including good continuity and conformality in aggressive device structures (devices with small feature size and deep trenching with high aspect ratios) in order to perform as a viable diffusion barrier. In addition, the barriers must be very thin in order to maintain the advantage of low effective resistance or capacitance achieved through combination of Cu and low-*k* materials.[1-3] The tradeoff between continuity and thickness places stringent requirements on barrier integrity and stability, especially in Cu/porous low-*k* integration schemes where the ability to form a continuous barrier layer may be greatly affected by the presence of porous structure underneath and its attendant surface roughness.[4] Hence, it is fundamentally important to understand the effects of such film properties as pore size and distribution, surface roughness, and processing procedures on barrier continuity. Most studies to date[5] have monitored electrical property degradation after integration processing without directly determining the underlying physical mechanisms involved. The simple reason for this is the relative shortage of analytical techniques for characterizing pores, thin-film continuity, and Cu diffusion, all at the 1-10 nm scale.

In the last several years positronium annihilation lifetime spectroscopy (PALS) has become an established technique for probing nanoporous structures.[6-9] More recently, we have shown the sensitivity of PALS to Cu interdiffusion and demonstrated how to use PALS to determine whether a diffusion barrier on an open-pored low-*k* film is continuous.[10] PALS can detect nanopore sizes and distributions by correlating the annihilation decay lifetime of positronium (Ps, the electron bound state with its antiparticle, the positron) with the dimensions of closed pores.[11] In interconnected pores, however, Ps can diffuse over long distances (on the order of micrometers[7]) within the interconnected porous network and can often easily escape from the film into vacuum. Ps diffusion is illustrated schematically in Fig. 1a. The detection of copious Ps in vacuum signals interconnected film porosity and the presence of open paths in the surface region to the vacuum system. Such escaping of Ps can be prevented by a continuous top layer, an effective Ps diffusion barrier (Fig. 1b). It has been observed that small pinholes or discontinuities in the barrier itself (Fig. 1c) can form a passage allowing Ps to escape into vacuum, which can easily be detected by PALS.[10] It was also found that the pinholes or discontinuities that allow Ps to escape into vacuum are very likely to form open passages through which Cu atoms (or ions) can penetrate readily into the dielectric and degrade the electrical properties. Fortunately, possible Cu diffusion through a discontinuous barrier into a porous low-*k* (with interconnected pores) film can be correlated with easily detectable Ps vacuum signals in PALS.

In this work, we use the methodology developed in our previous work[10] to explore the interrelated effects of pore size and low-*k* film surface roughness on diffusion barrier continuity. From previous work,[10] we found that Ta is more effective as a diffusion barrier than TaN; thus, Ta is chosen in this paper. PALS is used to determine the minimum thickness of Ta required to form an effective diffusion barrier on a series of chemically similar films where the average film pore size can be systematically varied. In addition, we find that the minimum thickness of Ta to form an effective diffusion barrier also depends on film roughness as well as pore size. To complement and compare with PALS, atomic force microscopy (AFM) has been used on each film as a measure of surface roughness. Our goal is to understand these structural effects on barrier continuity, which should enable one to control or optimize the materials and/or processing in order to minimize barrier thickness as required for advanced integrated circuits.[3]

Experimental

A series of blanket nanoporous XLK films on silicon wafers were supplied by Dow Corning Corporation. The thin films are processed by spin-coating a solution onto a silicon wafer, treating the as-spun film with moist ammonia, and then thermally curing the film. The initial solution was comprised of hydrogen silsesquioxane resin and two solvents. Methyl propyl ketone, a low-boiling solvent, was used to control the thickness of the as-spun film. The second solvent, tetradecane, which has a high boiling point, remained with the resin in the as-spun film. The ratio of the resin to high-boiling solvent tetradecane is adjusted to control the porosity and hence the dielectric constant of the film (and the average pore size). After spin-coating, the as-spun film was exposed to moist ammonia to cause the film to gel in the presence of the tetradecane solvent. A hot-plate step of 150°C is used to evaporate the low-boiling-point methyl propyl ketone solvent. The remaining tetradecane was then removed by subsequent heating steps, which included a final cure in the range 400-450°C. These films are about 1 μm thick, with dielectric constant (*k*) varying from 1.5 to 2.5.

All the XLK films have interconnected pores as observed by the copious escape of Ps into vacuum. In order to enable PALS measurement of average pore sizes, capping layers on these films are required. A capped specimen for each sample was prepared by uniformly depositing a 100 nm thick layer of silicon oxide on the surface. Candidate Ta diffusion barrier layers of 5, 15, and 25 nm thick

[z] E-mail: gidley@umich.edu

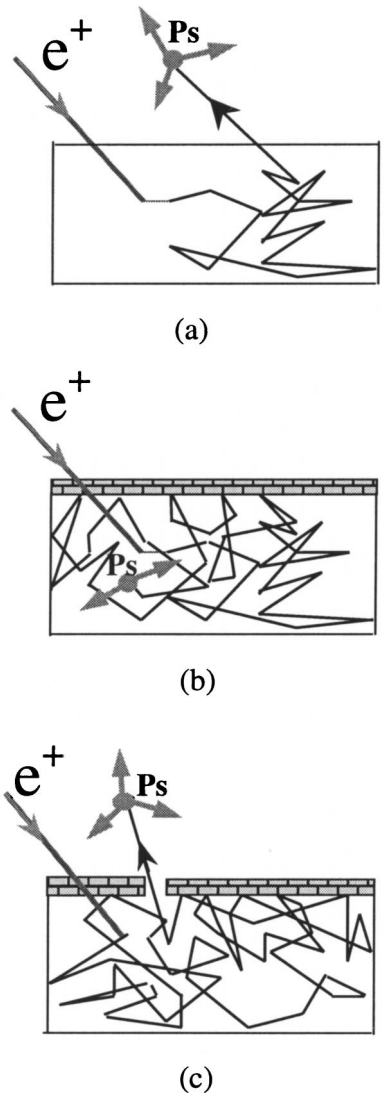

Figure 1. Ps behavior in barriered porous low-*k* films with interconnected porosity: (a) no barrier, (b) an effective barrier, (c) a barrier with pinholes or discontinuities.

were sputter-deposited onto the XLK films in Ar with 7 mTorr total gas pressure using an Ener-Jet Sputter Coater. To compare the effect of surface roughness on barrier continuity, we have also investigated a porous Nanoglass A10C film, supplied by International Sematech.[10] Ta diffusion barriers of 25 and 35 nm were sputter-deposited on this film. The surface roughness on each uncapped and unbarriered low-*k* film was measured using a Digital Instruments NanoScope III AFM. A 1 × 1 μm area was scanned using the tapping mode.

A detailed instrument setup and the measurement methods of the PALS technique appear elsewhere.[6,7,10] PALS spectra with 10^7 events were acquired at room temperature with a positron beam and fast lifetime system with a resolution of ~500 ps. The Fortran program POSFIT was used for lifetime fitting.

Results and Discussion

A typical PALS spectrum acquired at a positron beam implantation energy of 5 keV using an uncapped XLK film is plotted in Fig. 2. The prompt peak is a convolution of fast positron and Ps decay, which does not provide information about the nanoporous structure in these materials and is neglected in the following discussion. The only signal of interest in these films is due to the copious Ps (20-30%) that annihilates with a vacuum lifetime about 140 ns. This unusually high vacuum Ps intensity indicates that there are highly interconnected pores that provide a readily accessible diffusion path into vacuum. A capping layer is required to prevent such escape of Ps by sealing off the open paths to vacuum.

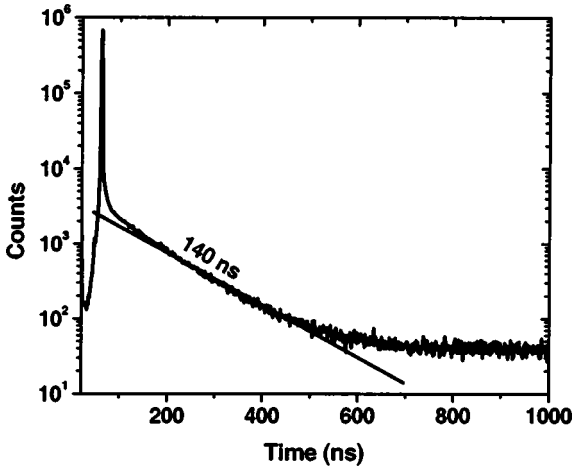

Figure 2. A typical PALS spectrum of the uncapped XLK films where virtually all the Ps decays with a single lifetime close to the vacuum value of 140 ns.

The annihilation lifetime spectra of the capped samples are plotted in Fig. 3. They typically require two long-lived Ps components for acceptable fitting, as shown in the inset of this figure. Only a small fraction of Ps annihilates with the vacuum lifetime of 140 ns (Fig. 4), which is due to electron capture by backscattered positrons from the incident beam. Such ''backscattered Ps'' is an ever-present effect when using positron beams and is present in the uncapped films as well but hidden in the high vacuum intensity of escaping Ps. The second component of Ps annihilating in the capped film has an intermediate lifetime, which is the intrinsic lifetime of Ps confined to the nanopores, as plotted in Fig. 5. These lifetimes are significantly reduced from the Ps vacuum lifetime and are correlated with the average pore sizes. Since the pores are highly interconnected, we use an infinitely long cylindrical pore model to deduce pore diameter (one possible visualization of such an interconnected network is illustrated in Fig. 6). According to the extended Tao-Eldrup model,[11] the average pore diameters are determined and plotted in Fig. 7. As can be seen, there is a clear trend between pore sizes and dielectric

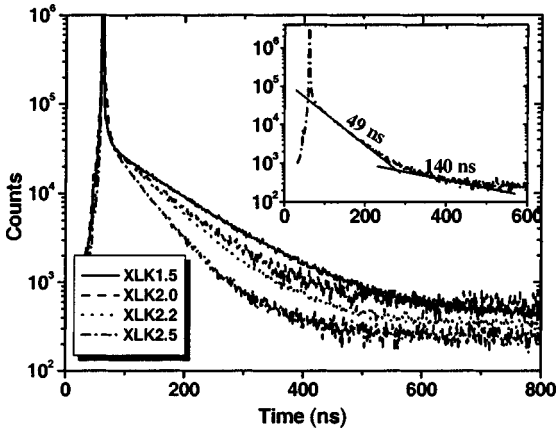

Figure 3. PALS spectra of capped XLK films. The inset spectrum of XLK2.5 is presented as an example to show that an intermediate lifetime component is required for acceptable fitting in the spectra of the capped films.

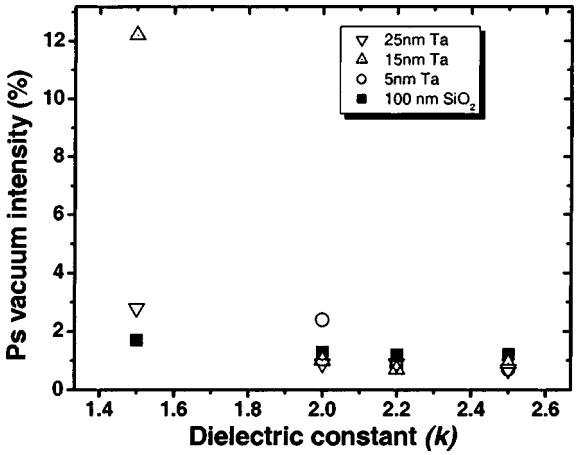

Figure 4. Ps vacuum intensity in the capped (100 nm SiO_2) and Ta-barriered XLK blanket films at 5.0 keV beam energy.

constant values. High-*k* and hence low porosity films tend to have small pores. Because all these films are made from the same procedure, varying only the porosity and the pore sizes, other material and/or process-dependent factors that can affect the continuity of the diffusion barrier, such as wettability of the barrier material to the low-*k* films, are considered to be similar for all the films.

The Ps vacuum intensities and Ps film lifetimes at 5.0 keV of the barriered films, along with the corresponding values determined in the capped films, are plotted in Fig. 4 and 5. The vacuum intensities of Ps in the XLK2.2 and XLK2.5 films (average pore diameter 3.8 and 2.7 nm, respectively) are consistent with that of backscattered Ps as determined from the capped films, even though only 5 nm Ta was deposited as the barrier layer. The Ps lifetimes measured in the mesopores agree with those determined in the capped films. All these results indicate that a 5 nm Ta barrier is thick enough to form a continuous layer on XLK2.2 and XLK2.5 and no structural pore change evidenced by any change in Ps lifetime is observed. Therefore, we can draw the conclusion that the minimum barrier thickness is no more than 5 nm for these two films. We do not consider thinner barriers at this point.

A Ta barrier only 5 nm thick, however, is not found to be completely effective in preventing Ps diffusion out of the XLK2.0 film, which has an average pore diameter of 4.5 nm. The Ps vacuum intensity of this film (Fig. 4) is about twice as high as that expected just from backscattered Ps. We believe that there must be some pinholes or discontinuities in the barrier layer. With a thermal velocity of 3×10^6 cm/s, Ps will have an average diffusion length of several micrometers in interconnected pores and make tens of thousands of attempts to probe the surface region within its lifetime. It can be very sensitive to any pinholes or discontinuities in the barrier layer[10] and can signal their presence by the escape of Ps (Fig. 1c), which is readily manifested by a telltale 140 ns component in the fitted PALS spectrum. The existence of open paths for Ps to escape through the Ta barrier layer is further supported by the reduced fitted Ps film lifetime shown in Fig. 5. It is generally found that a reduced Ps lifetime is fitted when Ps can escape into vacuum.[12] All these factors point to the conclusion that the 5 nm Ta barrier is not continuous on the XLK2.0 film. When the barrier becomes 15 or 25 nm thick, no escaped Ps is detected and the Ps lifetime is equally as long as that of the oxide capped film. This indicates the formation of a continuous layer, which prevents any Ps atoms from escaping into vacuum despite their many collisions with the barrier. Therefore, we conclude that the minimum Ta barrier thickness for the XLK2.0 film lies between 5 and 15 nm.

The most obvious feature in Fig. 4 is the extraordinarily high vacuum intensity of Ps in the 15 nm Ta-barriered XLK1.5 film. The barrier is clearly not continuous on this film, which has the largest pores (7 nm) of these XLK films. When 25 nm Ta is deposited onto this film, the vacuum intensity of Ps is only slightly higher than that of backscattered Ps and the Ps film lifetime is marginally lower than that determined in the oxide-capped film. There could be small

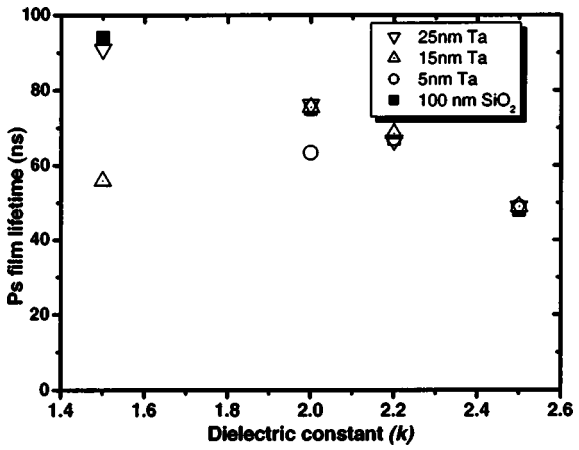

Figure 5. Fitted Ps film lifetime in the capped and Ta-barriered XLK films at 5.0 keV beam energy.

Figure 6. One possible example of a highly interconnected porous network which can be reasonably well characterized by an average tubular pore diameter.

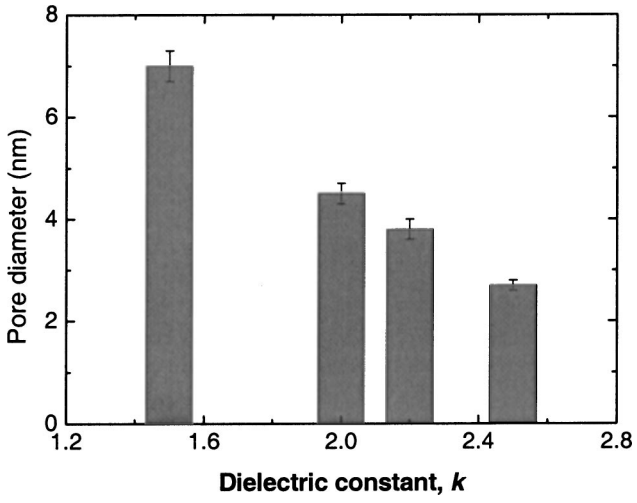

Figure 7. A trend between pore size and dielectric constant is observed in XLK films. Note the dielectric constant values were determined in the uncapped samples.

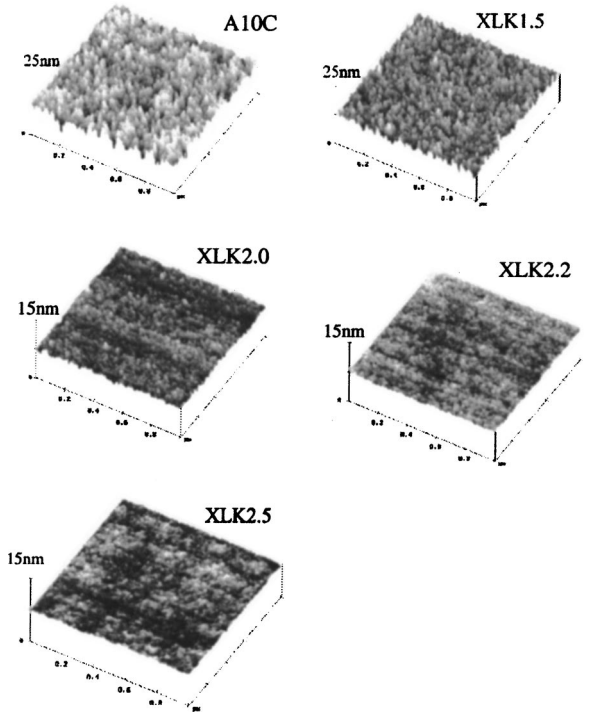

Figure 8. AFM images of the A10C film and the XLK series of films. Notice the difference in the scales. The depth scale of A10C and XLK1.5 is 25 nm whereas it is 15 nm for the other three films.

amounts of Ps leaking into the vacuum through defects in the barrier layer. Although the 25 nm Ta barrier may still not be perfectly continuous as a diffusion barrier, it dramatically improves the continuity compared to the thinner 15 nm barrier. We believe 25 nm is a lower bound on (and very close to) the minimum barrier thickness required for XLK1.5 film. These results indicate that pore size can affect the minimum barrier thickness. Not surprisingly, thick diffusion barriers tend to be required for films with large pores in order to form a continuous and effective barrier layer.

Similar experimental analyses have been made on Nanoglass A10C films.[10] PALS results indicate that the porous film has highly interconnected pores and the average pore diameter is 7 nm, about the same as that of XLK 1.5. After depositing 25 nm of Ta on top of the porous A10C, we find almost all the Ps still escapes into vacuum, which indicates that this barrier is far from being continuous. (In fact, pinholes have been observed in the 25 nm thick Ta barrier.[10]) This result contrasts with the XLK 1.5 film results where 25 nm Ta was nominally the minimum critical thickness. In this case we suspect that differences in the surface roughness may produce the disparate results.

AFM tests were performed on the surface of the A10C and XLK films and the 3-dimensional surface images are presented in Fig. 8. The average root-mean-square (rms) roughness and the maximum roughness of each film are listed in Table I. The histograms of peak height profile obtained from the AFM images are shown in Fig. 9. The A10C film has the roughest surface of all the films. The peaks spread in a wider range of height compared to those in the image of the XLK1.5 film. A good fraction of peaks are in the range 4-25 nm in height. A small but noticeable fraction of the peaks exceeds 25 nm in the A10C film. Indeed, a barrier of 35 nm is required to cap this film.[10] The peaks in the XLK1.5 film are normally distributed from 5 to 15 nm in height with tails on both sides, and PALS has observed Ps leakage in this film with a 15 nm Ta barrier. It appears that the height/depth of the peaks/valleys at the extreme end of the profile affect the barrier layer continuity (as monitored by escaping Ps), even if they occupy only a small fraction of the surface area.

Table I. The rms roughness and maximum roughness of porous low-*k* films determined by AFM.

Low-*k* film	Dielectric constant, *k*	Average pore diameter (nm)	rms roughness (nm)	Maximum roughness (nm)
A10C	2.2	7.0	3.0	28.8
XLK1.5	1.5	7.0	2.0	18.3
XLK2.0	2.0	4.5	0.9	7.9
XLK2.2	2.2	3.8	0.4	4.0
XLK2.5	2.5	2.7	0.5	3.7

Assuming uniform deposition, the barrier should not need to be thicker than the maximum depth, as can be naively perceived in the scenario of snow-covering mountains. However, the surface morphology can affect the ability of the barrier material to spread conformally on the surface area, especially in a physical vapor deposition (PVD) method such as sputter deposition. In general, it is difficult to completely cover a sharp and tall peak due to the high aspect ratio and the surface energy. This applies to the A10C film, which tends to have more numerous ''spiky'' peaks while the XLK films have relatively smoother surfaces and thinner minimum barrier thickness. Moreover, Ps with a lateral diffusion length on the order of a micrometer,[10,12] may have its vacuum escape probability saturate with only a few pinholes in an area of 1×1 μm (which is also the size of the AFM scanning region). Hence, PALS results may be dominated by the few largest peak-to-valley spots that are not clearly presented on the AFM roughness histogram. Furthermore, there is concern about the diffusion of barrier material into the porous films, especially with films possessing big, open pores, as has been observed in the A10C film.[10] In this case, the barrier appears to

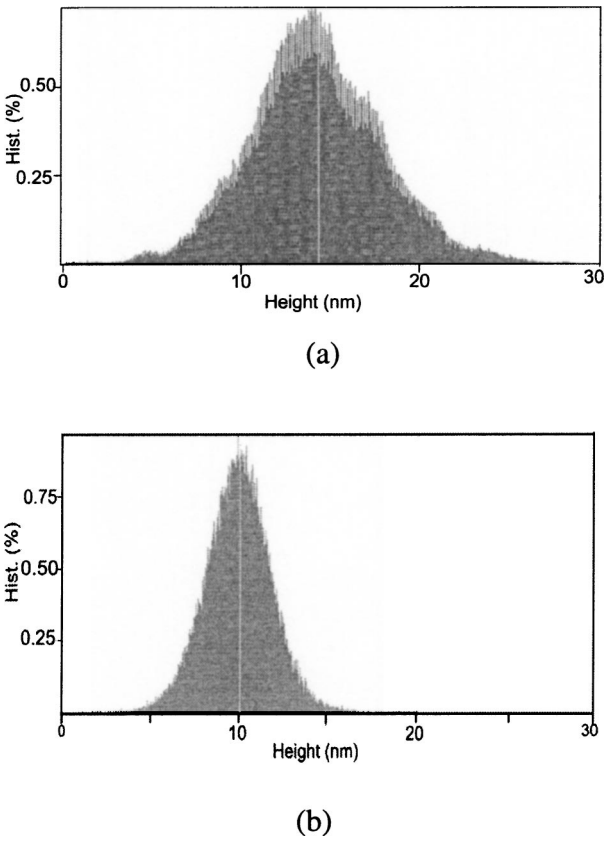

Figure 9. Histograms of peak height profile of (a) A10C and (b) XLK1.5 films based on their AFM images shown in Fig. 8.

be thinner locally and this could become a ''leaky'' spot for Ps to escape. Therefore, barrier layers are required to be at least thick enough to cover these deep valleys. As a matter of fact, we have observed herein that the minimum barrier layer thickness determined in PALS is equal to or larger than the maximum AFM-detected depth for each of the films.

Based on the discussion, it is clear that the surface roughness and average pore size indeed affect the minimum barrier layer thickness of films with interconnected porosity. Meanwhile, the surface roughness is also inherently correlated with the pore size, as we have seen with the XLK films. The films become rougher as the pore sizes grow and correspondingly, thicker layers are required to be effective, continuous barriers. Processes that can produce smaller pores and smoother film surfaces should be preferred to minimize the barrier layer. Deposition methods that can achieve better conformality can also be considered. Nevertheless, PALS provides a quick and straightforward check for candidate barrier materials and thicknesses.

Conclusions

We have studied diffusion barrier continuity on porous low-dielectric thin films with interconnected porosity. A series of Dow Corning XLK films are made from the same manufacturing procedures with different dielectric constants. Pore sizes are found to change inversely with the dielectric constant, while the minimum barrier layer thickness is found to increase with pore size. AFM analysis indicates that increasing pore size produces greater surface roughness, which by itself can have a dramatic influence on the barrier continuity after comparing the two films which have the same pore size. Thicker barriers are required in order to form a continuous, effective layer on a rougher surface with sharp peaks. This work should shed light on understanding the factors that can affect barrier efficacy in order to minimize diffusion barrier thickness and optimize device performance and reliability.

Acknowledgments

This work is supported by the National Science Foundation grant ECS-0100009, the Low-K Dielectric Program at International Sematech and Dow Corning, Incorporated. We would like to thank Dr. Albert Yee at IMRE, Singapore, for helpful discussions and Dr. Stella Pang at the University of Michigan for sputter deposition of Ta layers.

The University of Michigan assisted in meeting the publication costs of this article.

References

1. B. Zhao and M. Brongo, *Mater. Res. Soc. Symp. Proc.*, **565**, 137 (1999).
2. A. E. Kaloyeros and E. Eisenbraun, *Annu. Rev. Mater. Sci.*, **30**, 363 (2000).
3. Semiconductor Industry Association, International Technology Roadmaps of Semiconductors (1999).
4. E. T. Ryan, H.-M. Ho, W.-L. Wu, P. S. Ho, D. W. Gidley, and J. Drage, in *Proceedings of the International Interconnect Technology Conference*, San Francisco, CA, May 24-26, 1999, p. 187.
5. C. V. Nguyen, R. B. Beyers, C. J. Hawker, J. L. Hendrick, R. L. Jaffe, R. D. Miller, J. F. Remenar, H. W. Rhee, M. F. Toney, M. Trollsas, and D. Y. Yoon, *Polym. Prepr. (Am. Chem. Soc. Div. Polym. Chem.)*, **40**, 398 (1999).
6. D. W. Gidley, W. E. Frieze, T. L. Dull, J. N. Sun, A. F. Yee, C. V. Nguyen, and D. Y. Yoon, *Appl. Phys. Lett.*, **76**, 1282 (2000).
7. D. W. Gidley, W. E. Frieze, A. F. Yee, T. L. Dull, H.-M. Ho, and E. T. Ryan, *Phys. Rev. B, Rapid. Commun.*, **60**, R5157 (1999).
8. M. P. Petkov, M. H. Weber, K. G. Lynn, and K. P. Rodbell, *Appl. Phys. Lett.*, **77**, 2470 (2000).
9. D. W. Gidley, K. G. Lynn, M. P. Petkov, M. H. Weber, J. N. Sun, and A. F. Yee, in *New Directions in Antimatter Chemistry and Physics*, C. M. Surko and F. A. Gianturco, Editors, p. 151, Kluwer Academic, Netherlands (2001).
10. J. N. Sun, D. W. Gidley, T. L. Dull, W. E. Frieze, A. F. Yee, E. T. Ryan, S. Li, and J. Wetzel, *J. Appl. Phys.*, **89**, 5138 (2001).
11. T. L. Dull, W. E. Frieze, D. W. Gidley, J. N. Sun, and A. F. Yee, *J. Phys. Chem. B*, **105**, 4657 (2001).
12. J. N. Sun, Ph.D. Dissertation, The University of Michigan, Ann Arbor, MI (2002).